Search for $B^+ \to \tau^+ \nu$ decays with hadronic B tags

B. Aubert,[1] M. Bona,[1] D. Boutigny,[1] Y. Karyotakis,[1] J. P. Lees,[1] V. Poireau,[1] X. Prudent,[1] V. Tisserand,[1] A. Zghiche,[1] J. Garra Tico,[2] E. Grauges,[2] L. Lopez,[3] A. Palano,[3] M. Pappagallo,[3] G. Eigen,[4] B. Stugu,[4] L. Sun,[4] G. S. Abrams,[5] M. Battaglia,[5] D. N. Brown,[5] J. Button-Shafer,[5] R. N. Cahn,[5] Y. Groysman,[5] R. G. Jacobsen,[5] J. A. Kadyk,[5] L. T. Kerth,[5] Yu. G. Kolomensky,[5] G. Kukartsev,[5] D. Lopes Pegna,[5] G. Lynch,[5] L. M. Mir,[5] T. J. Orimoto,[5] I. L. Osipenkov,[5] M. T. Ronan,[5,*] K. Tackmann,[5] T. Tanabe,[5] W. A. Wenzel,[5] P. del Amo Sanchez,[6] C. M. Hawkes,[6] A. T. Watson,[6] H. Koch,[7] T. Schroeder,[7] D. Walker,[8] D. J. Asgeirsson,[9] T. Cuhadar-Donszelmann,[9] B. G. Fulsom,[9] C. Hearty,[9] T. S. Mattison,[9] J. A. McKenna,[9] M. Barrett,[10] A. Khan,[10] M. Saleem,[10] L. Teodorescu,[10] V. E. Blinov,[11] A. D. Bukin,[11] V. P. Druzhinin,[11] V. B. Golubev,[11] A. P. Onuchin,[11] S. I. Serednyakov,[11] Yu. I. Skovpen,[11] E. P. Solodov,[11] K. Yu. Todyshev,[11] M. Bondioli,[12] S. Curry,[12] I. Eschrich,[12] D. Kirkby,[12] A. J. Lankford,[12] P. Lund,[12] M. Mandelkern,[12] E. C. Martin,[12] D. P. Stoker,[12] S. Abachi,[13] C. Buchanan,[13] S. D. Foulkes,[14] J. W. Gary,[14] F. Liu,[14] O. Long,[14] B. C. Shen,[14] G. M. Vitug,[14] L. Zhang,[14] H. P. Paar,[15] S. Rahatlou,[15] V. Sharma,[15] J. W. Berryhill,[16] C. Campagnari,[16] A. Cunha,[16] B. Dahmes,[16] T. M. Hong,[16] D. Kovalskyi,[16] J. D. Richman,[16] T. W. Beck,[17] A. M. Eisner,[17] C. J. Flacco,[17] C. A. Heusch,[17] J. Kroseberg,[17] W. S. Lockman,[17] T. Schalk,[17] B. A. Schumm,[17] A. Seiden,[17] M. G. Wilson,[17] L. O. Winstrom,[17] E. Chen,[18] C. H. Cheng,[18] F. Fang,[18] D. G. Hitlin,[18] I. Narsky,[18] T. Piatenko,[18] F. C. Porter,[18] R. Andreassen,[19] G. Mancinelli,[19] B. T. Meadows,[19] K. Mishra,[19] M. D. Sokoloff,[19] F. Blanc,[20] P. C. Bloom,[20] S. Chen,[20] W. T. Ford,[20] J. F. Hirschauer,[20] A. Kreisel,[20] M. Nagel,[20] U. Nauenberg,[20] A. Olivas,[20] J. G. Smith,[20] K. A. Ulmer,[20] S. R. Wagner,[20] J. Zhang,[20] A. M. Gabareen,[21] A. Soffer,[21,†] W. H. Toki,[21] R. J. Wilson,[21] F. Winklmeier,[21] D. D. Altenburg,[22] E. Feltresi,[22] A. Hauke,[22] H. Jasper,[22] J. Merkel,[22] A. Petzold,[22] B. Spaan,[22] K. Wacker,[22] V. Klose,[23] M. J. Kobel,[23] H. M. Lacker,[23] W. F. Mader,[23] R. Nogowski,[23] J. Schubert,[23] K. R. Schubert,[23] R. Schwierz,[23] J. E. Sundermann,[23] A. Volk,[23] D. Bernard,[24] G. R. Bonneaud,[24] E. Latour,[24] V. Lombardo,[24] Ch. Thiebaux,[24] M. Verderi,[24] P. J. Clark,[25] W. Gradl,[25] F. Muheim,[25] S. Playfer,[25] A. I. Robertson,[25] J. E. Watson,[25] Y. Xie,[25] M. Andreotti,[26] D. Bettoni,[26] C. Bozzi,[26] R. Calabrese,[26] A. Cecchi,[26] G. Cibinetto,[26] P. Franchini,[26] E. Luppi,[26] M. Negrini,[26] A. Petrella,[26] L. Piemontese,[26] E. Prencipe,[26] V. Santoro,[26] F. Anulli,[27] R. Baldini-Ferroli,[27] A. Calcaterra,[27] R. de Sangro,[27] G. Finocchiaro,[27] S. Pacetti,[27] P. Patteri,[27] I. M. Peruzzi,[27,‡] M. Piccolo,[27] M. Rama,[27] A. Zallo,[27] A. Buzzo,[28] R. Contri,[28] M. Lo Vetere,[28] M. M. Macri,[28] M. R. Monge,[28] S. Passaggio,[28] C. Patrignani,[28] E. Robutti,[28] A. Santroni,[28] S. Tosi,[28] K. S. Chaisanguanthum,[29] M. Morii,[29] J. Wu,[29] R. S. Dubitzky,[30] J. Marks,[30] S. Schenk,[30] U. Uwer,[30] D. J. Bard,[31] P. D. Dauncey,[31] R. L. Flack,[31] J. A. Nash,[31] W. Panduro Vazquez,[31] M. Tibbetts,[31] P. K. Behera,[32] X. Chai,[32] M. J. Charles,[32] U. Mallik,[32] J. Cochran,[33] H. B. Crawley,[33] L. Dong,[33] V. Eyges,[33] W. T. Meyer,[33] S. Prell,[33] E. I. Rosenberg,[33] A. E. Rubin,[33] Y. Y. Gao,[34] A. V. Gritsan,[34] Z. J. Guo,[34] C. K. Lae,[34] A. G. Denig,[35] M. Fritsch,[35] G. Schott,[35] N. Arnaud,[36] J. Béquilleux,[36] A. D'Orazio,[36] M. Davier,[36] G. Grosdidier,[36] A. Höcker,[36] V. Lepeltier,[36] F. Le Diberder,[36] A. M. Lutz,[36] S. Pruvot,[36] S. Rodier,[36] P. Roudeau,[36] M. H. Schune,[36] J. Serrano,[36] V. Sordini,[36] A. Stocchi,[36] W. F. Wang,[36] G. Wormser,[36] D. J. Lange,[37] D. M. Wright,[37] I. Bingham,[38] J. P. Burke,[38] C. A. Chavez,[38] J. R. Fry,[38] E. Gabathuler,[38] R. Gamet,[38] D. E. Hutchcroft,[38] D. J. Payne,[38] K. C. Schofield,[38] C. Touramanis,[38] A. J. Bevan,[39] K. A. George,[39] F. Di Lodovico,[39] R. Sacco,[39] G. Cowan,[40] H. U. Flaecher,[40] D. A. Hopkins,[40] S. Paramesvaran,[40] F. Salvatore,[40] A. C. Wren,[40] D. N. Brown,[41] C. L. Davis,[41] J. Allison,[42] D. Bailey,[42] N. R. Barlow,[42] R. J. Barlow,[42] Y. M. Chia,[42] C. L. Edgar,[42] G. D. Lafferty,[42] T. J. West,[42] J. I. Yi,[42] J. Anderson,[43] C. Chen,[43] A. Jawahery,[43] D. A. Roberts,[43] G. Simi,[43] J. M. Tuggle,[43] G. Blaylock,[44] C. Dallapiccola,[44] S. S. Hertzbach,[44] X. Li,[44] T. B. Moore,[44] E. Salvati,[44] S. Saremi,[44] R. Cowan,[45] D. Dujmic,[45] P. H. Fisher,[45] K. Koeneke,[45] G. Sciolla,[45] M. Spitznagel,[45] F. Taylor,[45] R. K. Yamamoto,[45] M. Zhao,[45] Y. Zheng,[45] S. E. Mclachlin,[46,*] P. M. Patel,[46] S. H. Robertson,[46] A. Lazzaro,[47] F. Palombo,[47] J. M. Bauer,[48] L. Cremaldi,[48] V. Eschenburg,[48] R. Godang,[48] R. Kroeger,[48] D. A. Sanders,[48] D. J. Summers,[48] H. W. Zhao,[48] S. Brunet,[49] D. Côté,[49] M. Simard,[49] P. Taras,[49] F. B. Viaud,[49] H. Nicholson,[50] G. De Nardo,[51] F. Fabozzi,[51,§] L. Lista,[51] D. Monorchio,[51] G. Onorato,[51] C. Sciacca,[51] M. A. Baak,[52] G. Raven,[52] H. L. Snoek,[52] C. P. Jessop,[53] K. J. Knoepfel,[53] J. M. LoSecco,[53] G. Benelli,[54] L. A. Corwin,[54] K. Honscheid,[54] H. Kagan,[54] R. Kass,[54] J. P. Morris,[54] A. M. Rahimi,[54] J. J. Regensburger,[54] S. J. Sekula,[54] Q. K. Wong,[54] N. L. Blount,[55] J. Brau,[55] R. Frey,[55] O. Igonkina,[55] J. A. Kolb,[55] M. Lu,[55] R. Rahmat,[55] N. B. Sinev,[55] D. Strom,[55] J. Strube,[55] E. Torrence,[55] N. Gagliardi,[56] A. Gaz,[56] M. Margoni,[56] M. Morandin,[56] A. Pompili,[56] M. Posocco,[56] M. Rotondo,[56] F. Simonetto,[56] R. Stroili,[56] C. Voci,[56] E. Ben-Haim,[57] H. Briand,[57] G. Calderini,[57] J. Chauveau,[57] P. David,[57] L. Del Buono,[57] Ch. de la Vaissière,[57] O. Hamon,[57] Ph. Leruste,[57] J. Malclès,[57] J. Ocariz,[57] A. Perez,[57] J. Prendki,[57] L. Gladney,[58] M. Biasini,[59] R. Covarelli,[59] E. Manoni,[59] C. Angelini,[60] G. Batignani,[60] S. Bettarini,[60] M. Carpinelli,[60] R. Cenci,[60] A. Cervelli,[60] F. Forti,[60] M. A. Giorgi,[60] A. Lusiani,[60]

G. Marchiori,[60] M. A. Mazur,[60] M. Morganti,[60] N. Neri,[60] E. Paoloni,[60] G. Rizzo,[60] J. J. Walsh,[60] J. Biesiada,[61] P. Elmer,[61] Y. P. Lau,[61] C. Lu,[61] J. Olsen,[61] A. J. S. Smith,[61] A. V. Telnov,[61] E. Baracchini,[62] F. Bellini,[62] G. Cavoto,[62] D. del Re,[62] E. Di Marco,[62] R. Faccini,[62] F. Ferrarotto,[62] F. Ferroni,[62] M. Gaspero,[62] P. D. Jackson,[62] L. Li Gioi,[62] M. A. Mazzoni,[62] S. Morganti,[62] G. Piredda,[62] F. Polci,[62] F. Renga,[62] C. Voena,[62] M. Ebert,[63] T. Hartmann,[63] H. Schröder,[63] R. Waldi,[63] T. Adye,[64] G. Castelli,[64] B. Franek,[64] E. O. Olaiya,[64] W. Roethel,[64] F. F. Wilson,[64] S. Emery,[65] M. Escalier,[65] A. Gaidot,[65] S. F. Ganzhur,[65] G. Hamel de Monchenault,[65] W. Kozanecki,[65] G. Vasseur,[65] Ch. Yèche,[65] M. Zito,[65] X. R. Chen,[66] H. Liu,[66] W. Park,[66] M. V. Purohit,[66] R. M. White,[66] J. R. Wilson,[66] M. T. Allen,[67] D. Aston,[67] R. Bartoldus,[67] P. Bechtle,[67] R. Claus,[67] J. P. Coleman,[67] M. R. Convery,[67] J. C. Dingfelder,[67] J. Dorfan,[67] G. P. Dubois-Felsmann,[67] W. Dunwoodie,[67] R. C. Field,[67] T. Glanzman,[67] S. J. Gowdy,[67] M. T. Graham,[67] P. Grenier,[67] C. Hast,[67] W. R. Innes,[67] J. Kaminski,[67] M. H. Kelsey,[67] H. Kim,[67] P. Kim,[67] M. L. Kocian,[67] D. W. G. S. Leith,[67] S. Li,[67] S. Luitz,[67] V. Luth,[67] H. L. Lynch,[67] D. B. MacFarlane,[67] H. Marsiske,[67] R. Messner,[67] D. R. Muller,[67] C. P. O'Grady,[67] I. Ofte,[67] A. Perazzo,[67] M. Perl,[67] T. Pulliam,[67] B. N. Ratcliff,[67] A. Roodman,[67] A. A. Salnikov,[67] R. H. Schindler,[67] J. Schwiening,[67] A. Snyder,[67] D. Su,[67] M. K. Sullivan,[67] K. Suzuki,[67] S. K. Swain,[67] J. M. Thompson,[67] J. Va'vra,[67] A. P. Wagner,[67] M. Weaver,[67] W. J. Wisniewski,[67] M. Wittgen,[67] D. H. Wright,[67] A. K. Yarritu,[67] K. Yi,[67] C. C. Young,[67] V. Ziegler,[67] P. R. Burchat,[68] A. J. Edwards,[68] S. A. Majewski,[68] T. S. Miyashita,[68] B. A. Petersen,[68] L. Wilden,[68] S. Ahmed,[69] M. S. Alam,[69] R. Bula,[69] J. A. Ernst,[69] V. Jain,[69] B. Pan,[69] M. A. Saeed,[69] F. R. Wappler,[69] S. B. Zain,[69] M. Krishnamurthy,[70] S. M. Spanier,[70] R. Eckmann,[71] J. L. Ritchie,[71] A. M. Ruland,[71] C. J. Schilling,[71] R. F. Schwitters,[71] J. M. Izen,[72] X. C. Lou,[72] S. Ye,[72] F. Bianchi,[73] F. Gallo,[73] D. Gamba,[73] M. Pelliccioni,[73] M. Bomben,[74] L. Bosisio,[74] C. Cartaro,[74] F. Cossutti,[74] G. Della Ricca,[74] L. Lanceri,[74] L. Vitale,[74] V. Azzolini,[75] N. Lopez-March,[75] F. Martinez-Vidal,[75,||] D. A. Milanes,[75] A. Oyanguren,[75] J. Albert,[76] Sw. Banerjee,[76] B. Bhuyan,[76] K. Hamano,[76] R. Kowalewski,[76] I. M. Nugent,[76] J. M. Roney,[76] R. J. Sobie,[76] P. F. Harrison,[77] J. Ilic,[77] T. E. Latham,[77] G. B. Mohanty,[77] H. R. Band,[78] X. Chen,[78] S. Dasu,[78] K. T. Flood,[78] J. J. Hollar,[78] P. E. Kutter,[78] Y. Pan,[78] M. Pierini,[78] R. Prepost,[78] S. L. Wu,[78] and H. Neal[79]

(The *BABAR* Collaboration)

[1]*Laboratoire de Physique des Particules, IN2P3/CNRS et Université de Savoie, F-74941 Annecy-Le-Vieux, France*
[2]*Universitat de Barcelona, Facultat de Fisica, Departament ECM, E-08028 Barcelona, Spain*
[3]*Università di Bari, Dipartimento di Fisica and INFN, I-70126 Bari, Italy*
[4]*University of Bergen, Institute of Physics, N-5007 Bergen, Norway*
[5]*Lawrence Berkeley National Laboratory and University of California, Berkeley, California 94720, USA*
[6]*University of Birmingham, Birmingham, B15 2TT, United Kingdom*
[7]*Ruhr Universität Bochum, Institut für Experimentalphysik 1, D-44780 Bochum, Germany*
[8]*University of Bristol, Bristol BS8 1TL, United Kingdom*
[9]*University of British Columbia, Vancouver, British Columbia, Canada V6T 1Z1*
[10]*Brunel University, Uxbridge, Middlesex UB8 3PH, United Kingdom*
[11]*Budker Institute of Nuclear Physics, Novosibirsk 630090, Russia*
[12]*University of California at Irvine, Irvine, California 92697, USA*
[13]*University of California at Los Angeles, Los Angeles, California 90024, USA*
[14]*University of California at Riverside, Riverside, California 92521, USA*
[15]*University of California at San Diego, La Jolla, California 92093, USA*
[16]*University of California at Santa Barbara, Santa Barbara, California 93106, USA*
[17]*University of California at Santa Cruz, Institute for Particle Physics, Santa Cruz, California 95064, USA*
[18]*California Institute of Technology, Pasadena, California 91125, USA*
[19]*University of Cincinnati, Cincinnati, Ohio 45221, USA*
[20]*University of Colorado, Boulder, Colorado 80309, USA*
[21]*Colorado State University, Fort Collins, Colorado 80523, USA*
[22]*Universität Dortmund, Institut für Physik, D-44221 Dortmund, Germany*
[23]*Technische Universität Dresden, Institut für Kern- und Teilchenphysik, D-01062 Dresden, Germany*
[24]*Laboratoire Leprince-Ringuet, CNRS/IN2P3, Ecole Polytechnique, F-91128 Palaiseau, France*
[25]*University of Edinburgh, Edinburgh EH9 3JZ, United Kingdom*
[26]*Università di Ferrara, Dipartimento di Fisica and INFN, I-44100 Ferrara, Italy*
[27]*Laboratori Nazionali di Frascati dell'INFN, I-00044 Frascati, Italy*
[28]*Università di Genova, Dipartimento di Fisica and INFN, I-16146 Genova, Italy*
[29]*Harvard University, Cambridge, Massachusetts 02138, USA*
[30]*Universität Heidelberg, Physikalisches Institut, Philosophenweg 12, D-69120 Heidelberg, Germany*
[31]*Imperial College London, London, SW7 2AZ, United Kingdom*

^{32}University of Iowa, Iowa City, Iowa 52242, USA

^{33}Iowa State University, Ames, Iowa 50011-3160, USA

^{34}Johns Hopkins University, Baltimore, Maryland 21218, USA

^{35}Universität Karlsruhe, Institut für Experimentelle Kernphysik, D-76021 Karlsruhe, Germany

^{36}Laboratoire de l'Accélérateur Linéaire, IN2P3/CNRS et Université Paris-Sud 11, Centre Scientifique d'Orsay,
B. P. 34, F-91898 ORSAY Cedex, France

^{37}Lawrence Livermore National Laboratory, Livermore, California 94550, USA

^{38}University of Liverpool, Liverpool L69 7ZE, United Kingdom

^{39}Queen Mary, University of London, E1 4NS, United Kingdom

^{40}University of London, Royal Holloway and Bedford New College, Egham, Surrey TW20 0EX, United Kingdom

^{41}University of Louisville, Louisville, Kentucky 40292, USA

^{42}University of Manchester, Manchester M13 9PL, United Kingdom

^{43}University of Maryland, College Park, Maryland 20742, USA

^{44}University of Massachusetts, Amherst, Massachusetts 01003, USA

^{45}Massachusetts Institute of Technology, Laboratory for Nuclear Science, Cambridge, Massachusetts 02139, USA

^{46}McGill University, Montréal, Québec, Canada H3A 2T8

^{47}Università di Milano, Dipartimento di Fisica and INFN, I-20133 Milano, Italy

^{48}University of Mississippi, University, Mississippi 38677, USA

^{49}Université de Montréal, Physique des Particules, Montréal, Québec, Canada H3C 3J7

^{50}Mount Holyoke College, South Hadley, Massachusetts 01075, USA

^{51}Università di Napoli Federico II, Dipartimento di Scienze Fisiche and INFN, I-80126, Napoli, Italy

^{52}NIKHEF, National Institute for Nuclear Physics and High Energy Physics, NL-1009 DB Amsterdam, The Netherlands

^{53}University of Notre Dame, Notre Dame, Indiana 46556, USA

^{54}Ohio State University, Columbus, Ohio 43210, USA

^{55}University of Oregon, Eugene, Oregon 97403, USA

^{56}Università di Padova, Dipartimento di Fisica and INFN, I-35131 Padova, Italy

^{57}Laboratoire de Physique Nucléaire et de Hautes Energies, IN2P3/CNRS, Université Pierre et Marie Curie-Paris6,
Université Denis Diderot-Paris7, F-75252 Paris, France

^{58}University of Pennsylvania, Philadelphia, Pennsylvania 19104, USA

^{59}Università di Perugia, Dipartimento di Fisica and INFN, I-06100 Perugia, Italy

^{60}Università di Pisa, Dipartimento di Fisica, Scuola Normale Superiore and INFN, I-56127 Pisa, Italy

^{61}Princeton University, Princeton, New Jersey 08544, USA

^{62}Università di Roma La Sapienza, Dipartimento di Fisica and INFN, I-00185 Roma, Italy

^{63}Universität Rostock, D-18051 Rostock, Germany

^{64}Rutherford Appleton Laboratory, Chilton, Didcot, Oxon, OX11 0QX, United Kingdom

^{65}DSM/Dapnia, CEA/Saclay, F-91191 Gif-sur-Yvette, France

^{66}University of South Carolina, Columbia, South Carolina 29208, USA

^{67}Stanford Linear Accelerator Center, Stanford, California 94309, USA

^{68}Stanford University, Stanford, California 94305-4060, USA

^{69}State University of New York, Albany, New York 12222, USA

^{70}University of Tennessee, Knoxville, Tennessee 37996, USA

^{71}University of Texas at Austin, Austin, Texas 78712, USA

^{72}University of Texas at Dallas, Richardson, Texas 75083, USA

^{73}Università di Torino, Dipartimento di Fisica Sperimentale and INFN, I-10125 Torino, Italy

^{74}Università di Trieste, Dipartimento di Fisica and INFN, I-34127 Trieste, Italy

^{75}IFIC, Universitat de Valencia-CSIC, E-46071 Valencia, Spain

^{76}University of Victoria, Victoria, British Columbia, Canada V8W 3P6

^{77}Department of Physics, University of Warwick, Coventry CV4 7AL, United Kingdom

^{78}University of Wisconsin, Madison, Wisconsin 53706, USA

^{79}Yale University, New Haven, Connecticut 06511, USA

We present a search for the decay $B^+ \to \tau^+ \nu$ using 383×10^6 $B\bar{B}$ pairs collected at the $\Upsilon(4S)$ resonance with the *BABAR* detector at the SLAC PEP-II *B* Factory. We select a sample of events with one

---

*Deceased

†Now at Tel Aviv University, Tel Aviv, 69978, Israel

‡Also with Università di Perugia, Dipartimento di Fisica, Perugia, Italy

§Also with Università della Basilicata, Potenza, Italy

‖Also with Universitat de Barcelona, Facultat de Fisica, Departament ECM, E-08028 Barcelona, Spain

completely reconstructed tag B in a hadronic decay mode ($B^- \rightarrow D^{(*)0}X^-$), and examine the rest of the event to search for a $B^+ \rightarrow \tau^+ \nu$ decay. We identify the τ lepton in the following modes: $\tau^+ \rightarrow e^+ \nu \bar{\nu}$, $\tau^+ \rightarrow \mu^+ \nu \bar{\nu}$, $\tau^+ \rightarrow \pi^+ \bar{\nu}$, and $\tau^+ \rightarrow \pi^+ \pi^0 \bar{\nu}$. We find a 2.2$\sigma$ excess in data and measure a branching fraction of $\mathcal{B}(B^+ \rightarrow \tau^+ \nu) = (1.8^{+0.9}_{-0.8}(\text{stat.}) \pm 0.4(\text{bkg. syst.}) \pm 0.2(\text{other syst.})) \times 10^{-4}$. We calculate the product of the B meson decay constant f_B and $|V_{ub}|$ to be $f_B \cdot |V_{ub}| = (10.1^{+2.3}_{-2.5}(\text{stat.})^{+1.2}_{-1.5}(\text{syst.})) \times 10^{-4}$ GeV.

The study of the purely leptonic decay $B^+ \rightarrow \tau^+ \nu$ [1] is of particular interest because it is sensitive to the product of the B meson decay constant f_B, and the absolute value of Cabibbo-Kobayashi-Maskawa matrix element V_{ub} [2,3]. In the standard model (SM), the decay proceeds via quark annihilation into a W^+ boson, with a branching fraction given by

$$\mathcal{B}(B^+ \rightarrow \tau^+ \nu) = \frac{G_F^2 m_B m_\tau^2}{8\pi} \left[1 - \frac{m_\tau^2}{m_B^2} \right]^2 \tau_{B^+} f_B^2 |V_{ub}|^2,$$

(1)

where G_F is the Fermi constant, τ_{B^+} is the B^+ lifetime, and m_B and m_τ are the B^+ meson and τ lepton masses. Using $|V_{ub}| = (4.31 \pm 0.30) \times 10^{-3}$ from experimental measurements of semileptonic B decays [4] and $f_B = 0.216 \pm 0.022$ GeV from lattice QCD [5], the SM estimate of the branching fraction for $B^+ \rightarrow \tau^+ \nu$ is $(1.5 \pm 0.4) \times 10^{-4}$.

The process $B^+ \rightarrow \tau^+ \nu$ is also sensitive to extensions of the SM. For instance, in two-Higgs doublet models [6] and in the minimal supersymmetric extension of the standard model [7,8] it could be mediated by charged Higgs bosons. The branching fraction measurement can therefore also be used to constrain the parameter space of extensions to the SM.

The $B^+ \rightarrow \mu^+ \nu$ and $B^+ \rightarrow e^+ \nu$ decays are significantly helicity suppressed with respect to the $B^+ \rightarrow \tau^+ \nu$ channel. However, a search for $B^+ \rightarrow \tau^+ \nu$ is experimentally more challenging, due to the presence of multiple neutrinos in the final state, which makes the experimental signature less distinctive. In a previously published analysis using a sample of 383×10^6 $\Upsilon(4S) \rightarrow B\bar{B}$ decays, based on the reconstruction of a semileptonic B decay on the tag side, the *BABAR* collaboration set an upper limit $\mathcal{B}(B^+ \rightarrow \tau^+ \nu) < 1.7 \times 10^{-4}$ at the 90% confidence level (CL) [9]. The Belle Collaboration has reported evidence from a search for this decay and the branching fraction was measured to be $\mathcal{B}(B^+ \rightarrow \tau^+ \nu) = (1.79^{+0.56}_{-0.49}(\text{stat.})^{+0.46}_{-0.51} \times (\text{syst.})) \times 10^{-4}$ [10].

The data used in this analysis were collected with the *BABAR* detector at the PEP-II storage ring. The sample corresponds to an integrated luminosity of 346 fb^{-1} at the $\Upsilon(4S)$ resonance (on-resonance) and 36.3 fb^{-1} taken at 40 MeV below the $\Upsilon(4S)$ resonance (off-resonance). The on-resonance sample contains 383×10^6 $B\bar{B}$ decays. The detector is described in detail elsewhere [11]. Charged-particle trajectories are measured in the tracking system

composed of a five-layer silicon vertex detector and a 40-layer drift chamber, operating in a 1.5 T solenoidal magnetic field. A Cherenkov detector is used for $\pi - K$ discrimination, a CsI calorimeter for photon detection and electron identification, and the flux return of the solenoid, which consists of layers of steel interspersed with resistive plate chambers or limited streamer tubes, for muon and neutral hadron identification.

In order to estimate signal selection efficiencies and to study physics backgrounds, we use a *BABAR* Monte Carlo (MC) simulation based on GEANT4 [12]. In MC simulated signal events one B^+ meson decays to $\tau^+ \nu$ and the other into any final state. The $B\bar{B}$ and continuum MC samples are, respectively, equivalent to approximately 3 times and 1.5 times the accumulated data sample. Beam-related background and detector noise are taken from data and overlaid on the simulated events.

We reconstruct an exclusive decay of one of the B mesons in the event (tag B) and examine the remaining particle(s) for the experimental signature of $B^+ \rightarrow \tau^+ \nu$. In order to avoid experimenter bias, the signal region in data is blinded until the final yield extraction is performed.

The tag B candidate is reconstructed in the set of hadronic B decay modes $B^- \rightarrow D^{(*)0}X^-$ [1], where X^- denotes a system of charged and neutral hadrons with total charge -1 composed of $n_1 \pi^\pm$, $n_2 K^\pm$, $n_3 K_S^0$, $n_4 \pi^0$, where $n_1 + n_2 \leq 5$, $n_3 \leq 2$, and $n_4 \leq 2$. We reconstruct $D^{*0} \rightarrow D^0 \pi^0, D^0 \gamma$; $D^0 \rightarrow K^- \pi^+$, $K^- \pi^+ \pi^0$, $K^- \pi^+ \pi^- \pi^+$, $K_S^0 \pi^+ \pi^-$, and $K_S^0 \rightarrow \pi^+ \pi^-$. The kinematic consistency of tag B candidates is checked with the beam energy-substituted mass $m_{ES} = \sqrt{s/4 - \vec{p}_B^2}$ and the energy difference $\Delta E = E_B - \sqrt{s}/2$. Here $\sqrt{s}$ is the total energy in the $\Upsilon(4S)$ center-of-mass (CM) frame, and $\vec{p}_B$ and E_B denote, respectively, the momentum and energy of the tag B candidate in the CM frame. The resolution on ΔE is measured to be $\sigma_{\Delta E} = 10$–35 MeV, depending on the decay mode; we require $|\Delta E| < 3\sigma_{\Delta E}$. The purity $\mathcal{P}$ of each reconstructed B decay mode is estimated, using on-resonance data, as the ratio of the number of peaking events with $m_{ES} > 5.27$ GeV/c^2 to the total number of events in the same range. If multiple tag B candidates are reconstructed, the one with the highest purity $\mathcal{P}$ is selected. If more than one candidate with the same purity is reconstructed, the one with the lowest value of $|\Delta E|$ is selected. From the data set obtained as described above, we consider only those events in which the tag B is reconstructed in the decay

modes of highest purity $\mathcal{P}$. The set of decay modes used is defined by the requirement that the purity of the resulting sample is not less than 30%.

The background consists of $e^+ e^- \to q\bar{q}(q = u, d, s, c)$ events and other $\Upsilon(4S) \to B^0\bar{B}^0$ or B^+B^- decays in which the tag B candidate is misreconstructed using particles coming from both B mesons in the event. To reduce the $e^+ e^- \to q\bar{q}$ background, we require $|\cos\theta^*_{TB}| < 0.9$, where θ^*_{TB} is the angle in the CM frame between the thrust axis [13] of the tag B candidate and the thrust axis of the remaining reconstructed charged and neutral candidates.

In order to determine the number of correctly reconstructed B^+ decays, we classify the background events in four categories: $e^+ e^- \to c\bar{c}$; $e^+ e^- \to u\bar{u}, d\bar{d}, s\bar{s}$; $\Upsilon(4S) \to B^0\bar{B}^0$; and $\Upsilon(4S) \to B^+B^-$. The m_{ES} shapes of these background distributions are taken from MC simulation. The normalization of the $e^+ e^- \to c\bar{c}$ and $e^+ e^- \to u\bar{u}, d\bar{d}, s\bar{s}$ backgrounds is taken from off-resonance data, scaled by the luminosity and corrected for the different selection efficiencies evaluated with the MC. The normalization of the $B^0\bar{B}^0$, B^+B^- components are obtained by means of a χ^2 fit to the m_{ES} distribution in the data sideband region ($5.22 \text{ GeV}/c^2 < m_{ES} < 5.26 \text{ GeV}/c^2$). The number of background events in the signal region ($m_{ES} > 5.27 \text{ GeV}/c^2$) is extrapolated from the fit and subtracted from the data. We estimate the total number of tagged B's in the data to be $N_B = (5.92 \pm 0.11(\text{stat.})) \times 10^5$. Figure 1 shows the tag B candidate m_{ES} distribution, with the combinatorial background, estimated as the sum of the four components described above, overlaid.

After the reconstruction of the tag B meson, a set of selection criteria is applied to the rest of the event (recoil) in order to enhance the sensitivity to $B^+ \to \tau^+ \nu$ decays. We require the presence of only one well-reconstructed charged track (signal track) with charge opposite to that of the tag B. The signal track is required to have at least 12

hits in the drift chamber, momentum transverse to the beam axis, p_T, greater than 0.1 GeV/c, and the point of closest approach to the interaction point less than 10 cm along the beam axis and less than 1.5 cm transverse to it.

The τ lepton is identified in four decay modes constituting approximately 71% of the total τ decay width: $\tau^+ \to e^+ \nu\bar{\nu}$, $\tau^+ \to \mu^+ \nu\bar{\nu}$, $\tau^+ \to \pi^+ \bar{\nu}$, and $\tau^+ \to \pi^+ \pi^0 \bar{\nu}$. Particle identification criteria on the signal track are used to separate the four categories. The $\tau^+ \to \pi^+ \pi^0 \bar{\nu}$ sample is obtained by associating the signal track, identified as pion, with a π^0 reconstructed from a pair of neutral clusters with invariant mass between 0.115 and 0.155 GeV/c^2 and total energy greater than 250 MeV. In case of multiple $\pi^+ \pi^0$ candidates, the one with largest center-of-mass momentum $p^*_{\pi^+ \pi^0}$ is chosen.

We place a τ mode-dependent cut on $|\cos\theta^*_{TB}|$ to reduce the background due to continuum events and incorrectly reconstructed tag B candidates (combinatorial). The remaining sources of background consists of B^+B^- events in which the tag B meson was correctly reconstructed and the recoil contains one track and additional particles that are not reconstructed by the tracking detectors and calorimeter. MC simulation shows that 82% of this background is from semileptonic B decays.

We define the discriminating variable E_{extra} as the sum of the energies of the neutral clusters not associated with the tag B or with the signal π^0 from the $\tau^+ \to \pi^+ \pi^0 \bar{\nu}$ mode, and passing a minimum energy requirement. The required energy depends on the selected signal mode and on the calorimeter region involved and varies from 50 to 70 MeV. Signal events tend to peak at low E_{extra} values, whereas background events, which contain additional sources of neutral clusters, are distributed toward higher E_{extra} values.

Other variables used to discriminate between signal and background are the CM momentum of the signal candidates, the multiplicities of low p_T charged tracks and of π^0 candidates in the recoil, and the direction of the missing momentum four vector in the CM frame. For the $\tau^+ \to \pi^+ \pi^0 \bar{\nu}$ mode, we exploit the presence of the π^0 in the final state and the dominance of the decay through the ρ^+ resonance by means of the combined quantity $x_\rho = [(m_{\pi^+ \pi^0} - m_\rho)/(\Gamma_\rho)]^2 + [(m_{\gamma\gamma} - m_{\pi^0})/(\sigma_{\pi^0})]^2$, where $m_{\pi^+ \pi^0}$ is the reconstructed invariant mass of the $\pi^+ \pi^0$ candidate, $m_{\gamma\gamma}$ is the reconstructed invariant mass of the π^0 candidate, m_ρ and Γ_ρ are the nominal values [4] for the ρ mass and width, m_{π^0} is the nominal π^0 mass, and $\sigma_{\pi^0} = 8 \text{ MeV}/c^2$ is the experimental resolution on the π^0 mass determined from data.

We optimize the selection by maximizing $s/\sqrt{s + b}$ using the B^+B^- MC and signal MC, where b is the expected background from B^+B^- events and s is the expected number of signal events in the hypothesis of a branching fraction of 1×10^{-4}. The optimization is performed separately for each τ decay mode and with all the
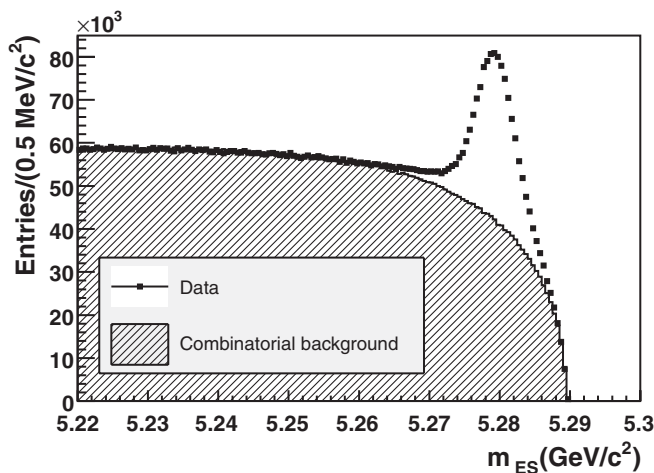

FIG. 1. Distribution of the energy-substituted mass, m_{ES}, of the tag B candidates in data. The combinatorial background is overlaid.

TABLE I.   Optimized selection criteria for each τ decay mode.

Variable	e^+	μ^+	π^+	$\pi^+\pi^0$
$E_{\rm extra}$(GeV)	<0.160	<0.100	<0.230	<0.290
π^0 multiplicity	0	0	≤ 2	$\cdots$
Track multiplicity	1	1	≤ 2	1
$|\cos\theta^*_{TB}|$	≤ 0.9	≤ 0.9	≤ 0.7	≤ 0.7
$p^*_{\rm trk}$(GeV/c)	<1.25	<1.85	>1.5	$\cdots$
$\cos\theta^*_{\rm miss}$	<0.9	$\cdots$	<0.5	<0.55
$p^*_{\pi^+\pi^0}$(GeV/c)	$\cdots$	$\cdots$	$\cdots$	>1.5
x_ρ	$\cdots$	$\cdots$	$\cdots$	<2.0
E_{π^0}(GeV)	$\cdots$	$\cdots$	$\cdots$	>0.250

cuts applied simultaneously in order to take into account any correlations among the discriminating variables. The optimized signal selection cuts are reported in Table I.

We compute the signal selection efficiency as the ratio of the number of signal MC events passing the selection criteria to the number of signal events that have a correctly reconstructed tag B candidate in the signal region $m_{\rm ES} > 5.27$ GeV/c^2. We evaluate the efficiencies on a signal MC sample which is distinct from the sample used in the optimization procedure. A small cross feed in some modes is estimated from MC and is taken into account in the computation of the total efficiency.

The total efficiency for each selection is given by

$$\varepsilon_i = \sum_{j=1}^{n_{\rm dec}} \varepsilon_i^j f_j, \qquad (2)$$

where ε_i^j is the efficiency of the selection i for the τ decay mode j, $n_{\rm dec}=7$ is the number of τ decay modes that can contribute to the reconstructed modes, and f_j are the fractions of the τ decay mode as estimated from the signal MC sample with a reconstructed tag B. Table II shows the estimated efficiencies.

TABLE II.   Efficiency (in percent) of the most relevant τ decay modes (rows) to be selected in one of the four modes considered in this analysis (column). The all decay row shows the selection efficiency of each reconstruction mode, adding the contribution from the previous rows, weighted by the decay abundance at the tag selection level f_j. The last row shows the total signal selection efficiency. The uncertainties are statistical only.

Mode	e^+	μ^+	π^+	$\pi^+\pi^0$
e^+	19.3 ± 1.1	0	0.4 ± 0.2	0
μ^+	0	10.8 ± 0.9	1.3 ± 0.3	0
π^+	0	0.1 ± 0.1	19.7 ± 1.3	0.5 ± 0.2
$\pi^+\pi^0$	0	0	1.5 ± 0.2	7.0 ± 0.5
$\pi^+\pi^+\pi^-$	0	0	0	0
$\pi^+\pi^0\pi^0$	0	0	0.2 ± 0.1	1.8 ± 0.4
Other	0	0	0.3 ± 0.2	0.1 ± 0.1
All dec. ϵ_i:	3.1 ± 0.2	1.7 ± 0.1	2.9 ± 0.2	2.2 ± 0.2
Total:		9.8 ± 0.3		

To determine the expected number of background events in the data, we use the final selected data samples with $E_{\rm extra}$ between 0 and 2.4 GeV. We first perform an extended unbinned maximum likelihood fit to the $m_{\rm ES}$ distribution in the $E_{\rm extra}$ sideband region 0.4 GeV $< E_{\rm extra} < 2.4$ GeV of the final sample. For the peaking component of the background we use a probability density function (PDF) which is a Gaussian function joined to an exponential tail (Crystal Ball function) [14]. As a PDF for the nonpeaking component, we use a phase space motivated threshold function (ARGUS function) [15]. From this fit, we determine a peaking yield $N_{\rm pk}^{\rm side,data}$ and signal shape parameters, to be used in later fits. We apply the same procedure to B^+B^- MC events which pass the final selection and determine the peaking yield $N_{\rm pk}^{\rm sideMC}$. To determine the MC peaking yield in the $E_{\rm extra}$ signal region $N_{\rm pk}^{\rm sig,MC}$, we fit $m_{\rm ES}$ in the $E_{\rm extra}$ signal region of the B^+B^- MC sample with the Crystal Ball parameters fixed to the values determined in the $E_{\rm extra}$ sideband fits described above. Analogously, we fit the $m_{\rm ES}$ distribution of data in the $E_{\rm extra}$ signal region to extract the combinatorial background $n_{\rm comb}$, evaluated as the integral of the ARGUS shaped component in the $m_{\rm ES} > 5.27$ GeV/c^2 region. We estimate the total expected background in the signal region as

$$b = \frac{N_{\rm pk}^{\rm sig,MC}}{N_{\rm pk}^{\rm side,MC}} \times N_{\rm pk}^{\rm side,data} + n_{\rm comb}. \qquad (3)$$

After finalizing the signal selection criteria, we measure the yield of events in each decay mode in on-resonance data. Table III reports the number of observed events together with the expected number of background events, for each τ decay mode. Figure 2 shows the $E_{\rm extra}$ distribution for data and expected background at the end of the selection. The signal MC, normalized to a branching fraction of 3×10^{-3} for illustrative purposes, is overlaid for comparison. The $E_{\rm extra}$ distribution is also plotted separately for each τ decay mode.

We combine the results on the observed number of events n_i and on the expected background b_i from each of the four signal decay modes ($n_{\rm ch}$) using the estimator $Q=\mathcal{L}(s+b)/\mathcal{L}(b)$, where $\mathcal{L}(s+b)$ and $\mathcal{L}(b)$ are the likelihood functions for signal plus background and

TABLE III.   Observed number of on-resonance data events in the signal region compared with the number of expected background events.

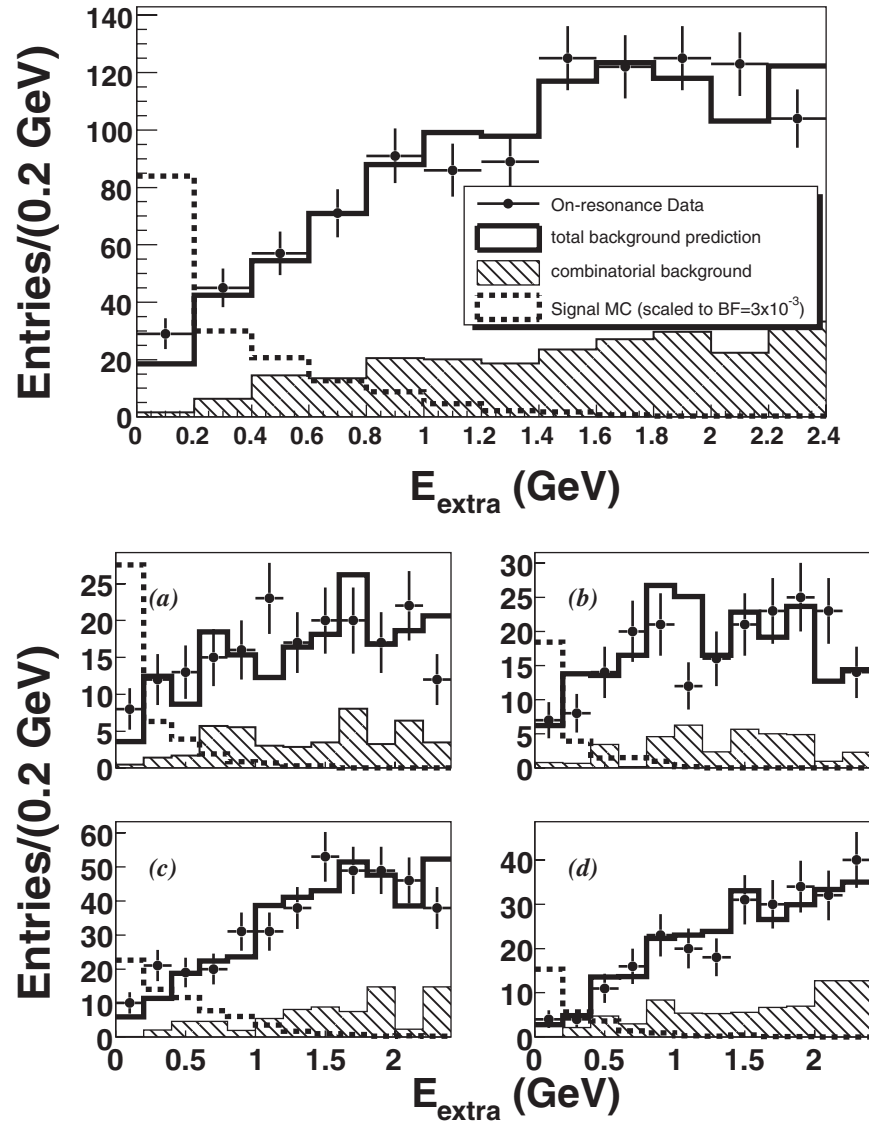| τ decay mode	Expected background	Observed
$\tau^+\to e^+\nu\bar\nu$	1.47 ± 1.37	4
$\tau^+\to\mu^+\nu\bar\nu$	1.78 ± 0.97	5
$\tau^+\to\pi^+\bar\nu$	6.79 ± 2.11	10
$\tau^+\to\pi^+\pi^0\bar\nu$	4.23 ± 1.39	5
All modes	14.27 ± 3.03	24

FIG. 2. E_{extra} distribution after all selection criteria have been applied. The upper plot shows the distribution of all the modes combined while lower plots show the (a) $\tau^+ \rightarrow e^+ \nu \bar{\nu}$, (b) $\tau^+ \rightarrow \mu^+ \nu \bar{\nu}$, (c) $\tau^+ \rightarrow \pi^+ \bar{\nu}$, and (d) $\tau^+ \rightarrow \pi^+ \pi^0 \bar{\nu}$ modes separately. The on-resonance data (black dots) distribution is compared with the total background prediction (continuous histogram). The hatched histrogram represents the combinatorial background component. $B^+ \rightarrow \tau^+ \nu$ signal MC (dashed histogram), normalized to a branching fraction of 3×10^{-3} for illustrative purposes, is shown for comparison.

background-only hypotheses, respectively

$$\mathcal{L}(s + b) \equiv \prod_{i=1}^{n_{\text{ch}}} \frac{e^{-(s_i + b_i)} (s_i + b_i)^{n_i}}{n_i!},$$

$$\mathcal{L}(b) \equiv \prod_{i=1}^{n_{\text{ch}}} \frac{e^{-b_i} b_i^{n_i}}{n_i!}. \tag{4}$$

The estimated number of signal candidates s_i in data, for each decay mode, is related to the $B^+ \rightarrow \tau^+ \nu$ branching fraction by

$$s_i = \frac{\varepsilon_{\text{sig}}^{\text{tag}}}{\varepsilon_B^{\text{tag}}} N_{B^+}^{\text{tag}} \varepsilon_i \mathcal{B}(B^+ \rightarrow \tau^+ \nu), \tag{5}$$

where $N_{B^+}^{\text{tag}}$ is the number of tag B^+ mesons correctly reconstructed, $\varepsilon_B^{\text{tag}}$ and $\varepsilon_{\text{sig}}^{\text{tag}}$ are the tag B efficiencies in generic $B\bar{B}$ and signal events, respectively, and ε_i are the signal efficiencies defined in Eq. (2). We fix the ratio $\varepsilon_{\text{sig}}^{\text{tag}}/\varepsilon_B^{\text{tag}} = 0.939 \pm 0.007(\text{stat.})$ to the value obtained from MC simulation.

We estimate the branching fraction (including statistical uncertainty and uncertainty from the background) by scanning over signal branching fraction hypotheses and com-

puting the value of $\mathcal{L}(s + b)/\mathcal{L}(b)$ for each hypothesis. The branching fraction is the hypothesis which minimizes the likelihood ratio $-2\ln Q = -2\ln(\mathcal{L}(s + b)/\mathcal{L}(b))$, and we determine the statistical uncertainty by finding the points on the likelihood scan that occur at one unit above the minimum.

The dominant uncertainty on the background predictions b_i is due to the finite B^+B^- MC statistics. We also check possible systematic effects in the estimation of combinatorial background by means of a sample of events with looser selection requirements; we find it to be negligible with respect to the statistical uncertainty. The background uncertainty is incorporated in the likelihood definition used to extract the branching fraction, by convolving it with a Gaussian function with standard deviation equal to the error on b_i [16].

The other sources of systematic uncertainty in the determination of the $B^+ \to \tau^+\nu$ branching fraction come from the estimation of the tag yield and efficiency and the reconstruction efficiency of the signal modes. We estimate the systematic uncertainty on the tag B yield and reconstruction efficiency by varying the MC B^+B^- nonpeaking component of the m_{ES} shape, assigning a systematic uncertainty of 3% on the branching fraction. The systematic uncertainties due to mismodeling of charged-particle tracking efficiency, E_{extra} shape, particle identification efficiency, π^0 reconstruction, and signal MC statistics depend on the τ decay mode. The uncertainty on the branching fraction is evaluated for each mode separately. We obtain the total contributions due to tracking and E_{extra} systematics by adding linearly the contributions of each decay channel. The total contributions due to MC statistics and particle identification are obtained by adding systematics uncertainties of each reconstruction mode in quadrature.

We check the low p_T charged track multiplicity distribution agreement between data and MC with a sample enriched in background by loosening the selection criteria. The disagreement, which is mode dependent, is quantified by comparing the MC PDF with the data PDF. We correct the MC to reproduce the distribution in data and apply the correction to the signal MC distribution. We take 100% of the correction as a systematic uncertainty, resulting in a total systematic uncertainty of 5.8% on the branching fraction.

The systematic uncertainty due to the E_{extra} mismodeling is determined by means of a data sample containing events with two nonoverlapping tag B candidates. The sample is selected by reconstructing a second B meson in a hadronic decay mode $B^- \to D^{(*)0}X^-$ on the recoil of the tag B. In addition to the requirements on the tag B described above, we consider only second B candidates satisfying $|\Delta E| < 50$ MeV and $m_{ES} > 5.27$ GeV/c^2 having opposite charge to that of the tag B. If multiple candidates are reconstructed, the one with the highest purity $\mathcal{P}$ is

TABLE IV. Contributions (in percent) to the systematic uncertainty on the branching fraction due to signal selection efficiency for different selection modes.

Source of systematics	e^+	μ^+	π^+	$\pi^+\pi^0$	Total
MC statistics	3.1	0.6	1.5	2.6	4.3
Particle Identification	1.5	1.3	0.2	0.2	2.0
π^0	$\cdots$	$\cdots$	$\cdots$	1.4	1.4
Tracking	3.7	0.4	0.1	1.6	5.8
E_{extra}	4.7	0.6	0.9	2.6	8.8
Signal B					11.6
Tag B					3
Total					12

selected. We compare the distribution of the total energy of the unassigned neutral clusters E_{extra} in data and in MC. We compute the ratio of the number of events in the signal region of each τ mode to the total number of events in the sample. For each τ mode, we evaluate the systematic uncertainty, comparing the ratio estimated from MC to the ratio estimated from data. This procedure results in a 8.8% systematic uncertainty on the branching fraction. Table IV shows the contributions in percent to the systematic uncertainties on the branching fraction.

In summary, we measure the branching fraction

$$\mathcal{B}(B^+ \to \tau^+\nu) = (1.8^{+0.9}_{-0.8} \pm 0.4 \pm 0.2) \times 10^{-4}, \quad (6)$$

where the first error is statistical, the second is due to the background uncertainty, and the third is due to other systematic sources. Taking into account the uncertainty on the expected background, as described above, we obtain a significance of 2.2σ.

Using Eq. (1), we calculate the product of the B meson decay constant f_B and $|V_{ub}|$ to be $f_B \cdot |V_{ub}| = (10.1^{+2.3}_{-2.5}(\text{stat.})^{+1.2}_{-1.5}(\text{syst.})) \times 10^{-4}$ GeV. We also measure the 90% CL upper limit using the CL_s method [17] to be $\mathcal{B}(B^+ \to \tau^+\nu) < 3.4 \times 10^{-4}$.

The combination of this measurement with the *BABAR* result obtained using semileptonic tags, based on a statistically independent data sample, and reported in [9], yields

$$\mathcal{B}(B^+ \to \tau^+\nu) = (1.2 \pm 0.4_{\text{stat.}} \pm 0.3_{\text{bkg.}} \pm 0.2_{\text{syst.}}) \times 10^{-4}. \quad (7)$$

The significance of the combined result is 2.6σ including the uncertainty on the expected background (3.2σ if this uncertainty is not included).

[1] Charge-conjugate modes are implied throughout the paper.

[2] N. Cabibbo, Phys. Rev. Lett. **10**, 531 (1963).

[3] M. Kobayashi and T. Maskawa, Prog. Theor. Phys. **49**, 652 (1973).

[4] W. M. Yao *et al.* (Particle Data Group), J. Phys. G **33**, 1 (2006).

[5] A. Gray *et al.* (HPQCD Collaboration), Phys. Rev. Lett. **95**, 212001 (2005).

[6] W. S. Hou, Phys. Rev. D **48**, 2342 (1993).

[7] G. Isidori and P. Paradisi, Phys. Lett. B **639**, 499 (2006).

[8] A. G. Akeroyd and C. H. Chen, Phys. Rev. D **75**, 075004 (2007).

[9] B. Aubert *et al.* (*BABAR* Collaboration), Phys. Rev. D **76**, 052002 (2007).

[10] K. Ikado *et al.* (Belle Collaboration), Phys. Rev. Lett. **97**, 251802 (2006).

[11] B. Aubert *et al.* (*BABAR* Collaboration), Nucl. Instrum. Methods Phys. Res., Sect. A **479**, 1 (2002).

[12] S. Agostinelli *et al.* (GEANT4 Collaboration), Nucl. Instrum. Methods Phys. Res., Sect. A **506**, 250 (2003).

[13] E. Farhi, Phys. Rev. Lett. **39**, 1587 (1977).

[14] M. J. Oreglia, Report No. SLAC-236, 1980; J. E. Gaiser, Report No. SLAC-255, 1982; T. Skwarnicki, Report No. DESY F31-86-02, 1986.

[15] H. Albrecht *et al.* (ARGUS Collaboration), Phys. Lett. B **185**, 218 (1987).

[16] C. Giunti, Phys. Rev. D **59**, 113009 (1999).

[17] A. L. Read, J. Phys. G **28**, 2693 (2002).